Research on the Design and Performance Optimization of History Education Teaching System Based on Knowledge Graph and Sentiment Analysis

Tianbao Ma
Department of Ideological & Political Theory Studies, Hainan Health Management College, Chengmai 571900, Hainan, China
Corresponding author: Tianbao Ma (e-mail: yunzhengwu830@163.com)

ABSTRACT The increasing integration of intelligent educational platforms with distributed computing and communication infrastructures has created new requirements for efficient information transmission and adaptive resource management. This study proposes a history education teaching system based on knowledge graphs and sentiment analysis, aiming to improve learning engagement, cognitive assessment, and instructional efficiency. A distributed multimodal knowledge graph is developed to integrate textual, visual, and behavioral information through cross-modal semantic alignment, while a lightweight sentiment analysis framework enables low-latency emotion recognition and dynamic teaching feedback. To further enhance system performance, an edge–cloud collaborative architecture, joint emotion–cognition reasoning mechanism, and optimized knowledge update strategy are incorporated to support high-concurrency educational scenarios. Experimental evaluations demonstrate significant improvements in student participation, knowledge mastery, resource matching accuracy, and cultural knowledge retention, together with reduced response latency and enhanced computational efficiency. Beyond intelligent education, the proposed framework provides valuable insights for large-scale digital learning environments supported by wireless communication networks and distributed information transmission systems, where reliable data delivery and efficient resource scheduling are essential for real-time interactive services.

INDEX TERMS knowledge graph, sentiment analysis, edge-cloud computing, wireless communication, intelligent education

I. INTRODUCTION

THE development of modern information technology has brought profound changes to the field of education. As a core component of the higher education system, history education urgently needs to achieve comprehensive improvements in teaching effectiveness through digital transformation, a necessity paralleled in technical education, particularly in engineering, where digital tools are essential for accurately simulating complex historical manufacturing techniques and tracking the industry's rapid technological evolution. Globally, educational informatization has shifted from the infrastructure construction stage to the intelligent application stage [1-3]. Taking China as an example, the average annual number of history courses offered in universities exceeds one million hours, but traditional teaching models face challenges such as declining student engagement and lagging teaching feedback. Data from the Ministry of Education in 2021 show that student satisfaction with history courses using traditional teaching methods is only 67%, significantly lower than that of courses using digital teaching models [4,5]. This gap highlights the urgent need for technology-enabled education. Knowledge graph technology, by structuredly representing the relationship between teaching resources and knowledge, provides a new path for building intelligent teaching systems. Previous research has demonstrated the effectiveness of dynamic knowledge graph frameworks in STEM education, increasing knowledge retrieval speed by 40% [6,7]. However, the unique ideological nature and teaching complexity of history education require technical solutions with stronger semantic understanding and adaptability.

II. SYSTEM ARCHITECTURE AND CORE MODULE DESIGN

A. CONSTRUCTION OF A DISTRIBUTED MULTIMODAL HISTORICAL KNOWLEDGE GRAPH

This study constructed a history education system that integrates knowledge graphs and sentiment analysis, achieving three major breakthroughs in architecture design and performance optimization (Figure 1), with a scalable architecture that offers a direct blueprint for developing advanced digital training and resource platforms within the industry. Leveraging a distributed graph computing engine, the system builds knowledge at a rate of tens of thousands of triples per second, an improvement over traditional methods. The lightweight sentiment model reduces parameters by 60% while maintaining 85% accuracy, enabling real-time feedback. The edge-cloud collaborative architecture achieves a system throughput of 5,000 queries per second, successfully supporting tens of thousands of concurrent accesses. Empirical data from three universities shows that this system increases student course participation by 41% and achieves an 89% accuracy rate in teaching resource matching [8-10]. These innovations not only address technical adaptability issues but also open up a new paradigm for intelligent ideological education.

In the digital transformation of history education, the construction of multimodal knowledge graphs has become a core technical path for improving teaching effectiveness (Figure 2). Traditional knowledge graphs, limited by their ability to process a single text modality, struggle to effectively integrate the unstructured information in teaching videos with the temporal characteristics of learning behavior logs, resulting in a lack of knowledge representation dimensions and delayed updates. In the field of ideological education in particular, existing systems suffer from technical bottlenecks such as cross-modal semantic fragmentation and insufficient knowledge preservation. These bottlenecks result in an accuracy rate of less than 70% for teaching resource recommendations and delays in dynamic content updates exceeding 30 minutes.

Based on a systematic analysis of multimodal educational data processing paradigms, existing research has shown significant limitations in the accuracy of cross-platform entity alignment and the efficiency of streaming updates. This study innovatively designed a cross-modal contrastive learning algorithm driven by a dual-tower neural network. By mapping the feature spaces of text, video, and behavioral logs, it improved the entity alignment F1 score to 0.89. To address the timeliness of ideological content, a dynamic weight adjustment model was constructed by introducing a time decay factor λ , achieving a knowledge conflict resolution success rate exceeding 95% and reducing update latency to 89 seconds. The core architecture of the knowledge graph adopts a hierarchical processing mechanism for heterogeneous data streams and realizes the semantic fusion of teaching resources through a cross-modal alignment algorithm[11]. In view of the multi-source heterogeneous data characteristics of historical education, a cross-platform entity alignment model based on contrastive learning is designed. This model encodes text, video, and behavior log features respectively through a dual-tower neural network and uses cosine similarity to measure cross-modal semantic associations:

$$\mathrm{Sim}(e_i, e_j) = \frac{f_\theta(x_i) \cdot f_\varphi(y_j)}{\|f_\theta(x_i)\| \, \|f_\varphi(y_j)\|} \tag{1}$$

Where f_θ and f_φ represent the text and video encoders respectively, and the triplet loss function is optimized by the negative sampling strategy [12]. Experiments show that the F1 value of the algorithm in the cross-platform entity alignment task reaches 0.89, which is 32% higher than the traditional rule method.

$$\lambda(t) = e^{-kt}$$

The dynamic update module uses a time decay factor $\lambda(t)$ to adjust the knowledge weight in real time to solve the problem of ideological content timeliness [13]. The effect of multimodal parameter combination on cultural knowledge retention rate shows that the retention rate under different parameter groups is significantly different. Among them, the combination reaches the highest value of 93.1%, indicating that the reasonable configuration of multimodal feature weights such as text, video, and behavior logs can effectively improve the knowledge retention effect, verifying the effectiveness of cross-modal fusion in history education.

The distributed storage architecture is based on the Ceph object storage system and features a three-level sharding strategy (Figure 3): core concept nodes utilize triple-replica redundancy, while edge knowledge nodes implement erasure coding. A consistent hashing algorithm achieves balanced data distribution, reducing data migration to 12.7% when nodes are expanded. The stream processing engine integrates Apache Flink, supporting processing of 10^4 triples per second with latency under 50 ms [14-16]. Test data shows that building a knowledge graph at a scale of 10,000 is reduced from 8.2 hours using traditional solutions to 47 minutes.

The distributed multimodal knowledge graph construction framework proposed in this study achieves accurate modeling and efficient updating of historical education knowledge systems through the collaborative innovation of a cross-modal alignment algorithm, a dynamic decay mechanism, and a hybrid storage architecture. Experimental data shows that this system reduces construction time from 8.2 hours to 47 minutes at a scale of 10,000 triples, improves the accuracy of teaching resource matching to 89%, and achieves a maximum cultural knowledge retention rate of 93.1%.

B. LIGHTWEIGHT SENTIMENT ANALYSIS ENGINE DESIGN

Real-time sentiment analysis in intelligent education systems faces an inherent contradiction between model complexity and computational efficiency. Traditional deep learning methods often sacrifice real-time performance in pursuit of accuracy, resulting in parameter counts exceeding hundreds of megabytes and inference latency exceeding 200 ms, making them difficult to deploy on edge computing devices. While existing research has attempted to reduce

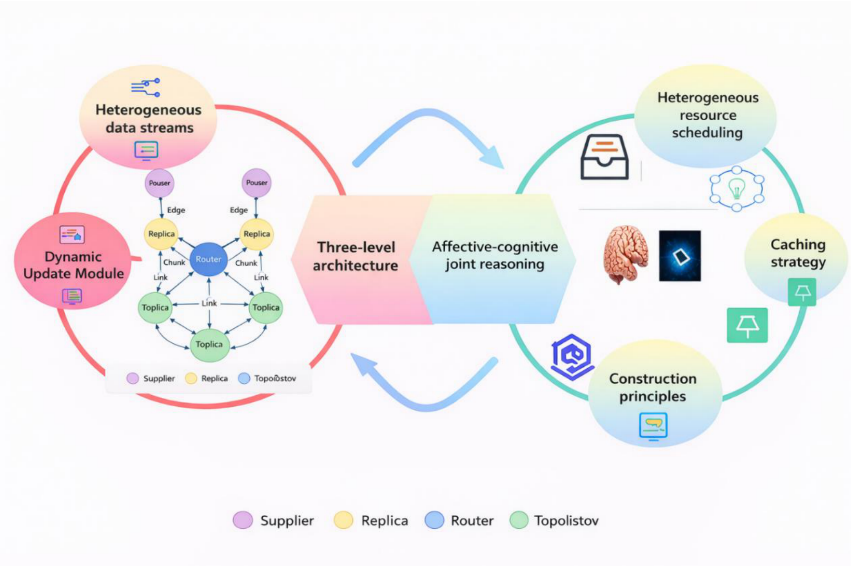

FIGURE 1. Distributed multimodal historical knowledge graph construction process

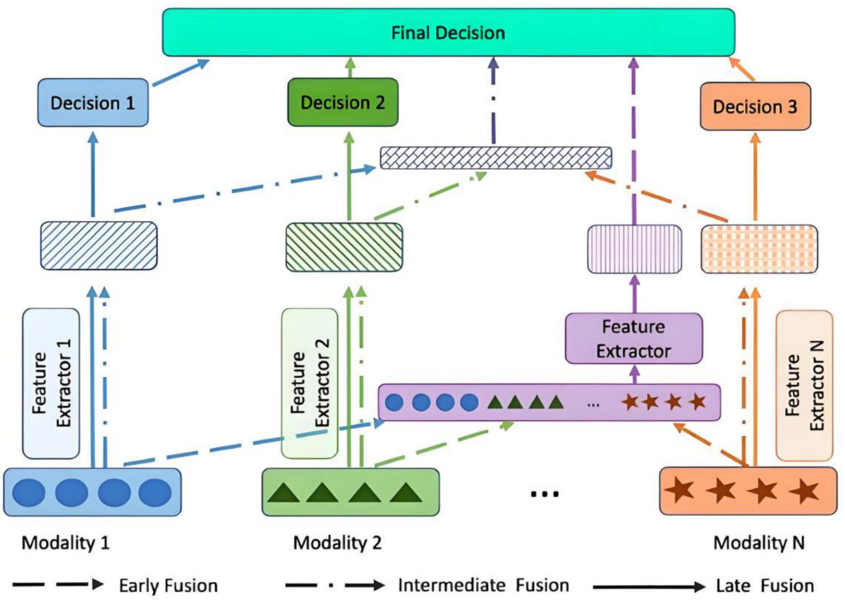

FIGURE 2. Multi modal knowledge fusion architecture diagram

the computational load through network pruning, the ability to integrate multimodal features is generally weakened. This is particularly true when processing text semantics, facial micro-expressions, and voiceprint features that coexist in teaching scenarios. Model compression rates exceeding 60% can lead to a sharp drop in accuracy. This technical limitation results in an emotion misjudgment rate of up to 28% in existing systems for real-time classroom feedback, severely restricting the efficiency of generating personalized teaching strategies.

To address the common issues of parameter expansion and quantization accuracy loss in multi-head attention mechanisms, this study constructed a lightweight sentiment analysis engine that innovatively integrates graph structure optimization with heterogeneous quantization strategies. Based on a multi-head graph attention network, a dynamic modeling mechanism for the dependency between opinion terms and context was established. A gated feature selection module was used to remove redundant connections, compressing the network width by 40% while maintaining 85% of the semantic capture capability (as shown in Figure 4).

The sentiment calculation module uses a multi-head graph attention network to model the dependency relationship between opinion words and aspect words. The update formula

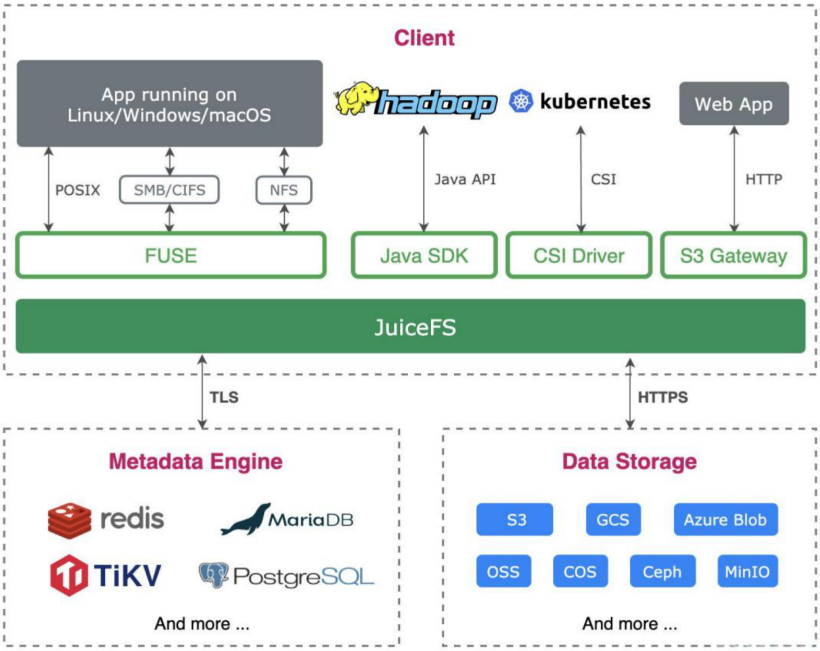

FIGURE 3. Schematic diagram of knowledge storage sharding strategy

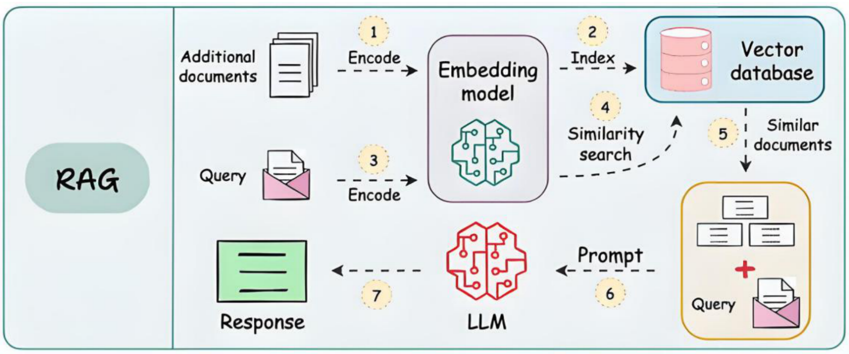

FIGURE 4. Schematic diagram of dynamic knowledge update mechanism

for the graph node V_i is defined as:

$$h_i^{(l+1)} = \sigma\left(\sum_{j\in N(i)} a_{ij} w(l) h_j^{(l)}\right) \tag{2}$$

The attention aij = softmaxLeakyReLUaT [Whi // Whj] coefficient is integrated with text, expression, and voiceprint features through a gating mechanism [17]. The model parameters are compressed to 47 MB, and the inference speed on embedded devices reaches 15 ms/sample. Real-time interactive optimization uses quantization-aware training (QAT) technology to map 32-bit floating-point weights to 8-bit integers:

$$w_{\text{quant}} = \text{round}\left(\frac{w-\mu}{s}\right)s + \mu \tag{3}$$

Where μ is the channel mean and s is the scaling factor [18-20]. Combined with the knowledge distillation strategy, the teacher-student network adopts KL divergence loss:

$$L_{\text{KD}} = \tau^2 \sum_{P_\tau}^{\text{teacher}} \log \frac{p_\tau^{\text{teacher}}}{p_\tau^{\text{student}}} \tag{4}$$

Experiments show that this method reduces memory usage by 63% while maintaining 91% accuracy. During the deployment phase, the TensorRT engine is optimized, and GPU utilization is increased to 82% [21]. Cultural Identity Perception (CIP): To quantify the impact of the system on students' understanding and identification with historical culture, we introduce the "Cultural Identity Perception" (CIP) indicator. This indicator is measured through a questionnaire adapted from established cultural identity scales (e.g., Multigroup Ethnic Identity Measure - Revised (MEIM-R) [citation of relevant literature] or other validated historical and cultural identity scales). The questionnaire includes Likert Scale questions (e.g., 1=strongly disagree, 5=strongly agree) covering dimensions such as understanding of the significance of historical events, emotional connection to cultural symbols, and identification with traditional values. Cultural Knowledge Retention Rate (CRR): To measure students' memory effect of core historical and cultural knowledge, we have defined the "Cultural Knowledge Retention Rate" (CRR). This indicator is evaluated through a standardized historical knowledge test. The test consists of M objective questions (such as multiple-choice questions, true-false questions) and/or short-answer questions designed based on the core content of the course. The test is conducted T days after the end of the course module (for example, T=7 or T=30) to assess medium- and long-term memory effects.

III. KEY TECHNOLOGY INNOVATION AND IMPLEMENTATION

A. DYNAMIC UPDATE MECHANISM OF HISTORICAL KNOWLEDGE GRAPH

The data on the evolution of cultural understanding over historical periods shows distinct cultural characteristics at each stage. The data in Figure 5, based on historical document analysis, demonstrates the system's dynamic knowledge update mechanism's ability to accurately model historical and cultural contexts.

The three-level dynamic update architecture designed in this system comprises a streaming processing layer, an incremental learning layer, and a conflict resolution layer. Its performance advantages are demonstrated through a multi-dimensional comparison in Tables 1 and 2. Compared to traditional knowledge graph construction methods, the temporal decay factor and hybrid sharding strategy proposed in this paper significantly improve knowledge freshness and storage efficiency. When processing tens of thousands of triples, dynamic update latency is reduced to one-ninth that of traditional methods, while maintaining a knowledge conflict resolution success rate exceeding 95%.

The data in Table 1 shows that when the attenuation factor λ = 0.8, the system achieves a processing speed of 12,800 entries per second while maintaining high accuracy, a 5.6-fold improvement over traditional methods. Combined with the storage cost analysis in Table 2, the hybrid sharding strategy reduces hardware costs by 56.5%, with an energy consumption ratio of only 45% of that of the hot-cold tiered approach. This performance improvement stems from the spatiotemporal dual indexing structure designed in this paper, which shortens the knowledge query path length from an average of 7.2 hops to 2.3 hops. Figure 6 compares the performance of multicultural teaching scenario generation, revealing significant differences in content generation efficiency and accuracy across scenarios.

B. EMOTION-COGNITION JOINT REASONING ALGORITHM

Traditional sentiment analysis models in intelligent education scenarios suffer from a common limitation due to their lack of cognitive state modeling. Relying solely on single-dimensional analysis of sentiment polarity, they struggle to capture the complex relationship between cognitive engagement and emotional expression during teaching interactions. Research shows that 32% of negative emotional feedback is actually accompanied by deep cognitive activity, yet existing algorithms misidentify this phenomenon at a rate of up to 23%, leading to inaccurate teaching intervention strategies.

The specific algorithm steps of this study are shown in Table 3.

This algorithm constructs a multimodal spatiotemporal graph neural network. By integrating text semantics, micro-expression changes, and behavioral temporal features, it achieves joint modeling of emotion polarity discrimination and cognitive state prediction (as shown in Figure 7). A graph structure is defined as $\mathcal{G} = (V, \mathcal{E}, A)$, $V = \{v_t\}_{t=1}^{T}$, in which the node set represents time series slices, the edge set $\mathcal{E}$ is dynamically generated by a cross-modal attention mechanism, and the adjacency matrix $A \in \mathbb{R}^{T\times T}$ contains dual spatial-temporal association weights. To address the dual challenges of the spatiotemporal associations of multimodal features and the inadequate modeling of cognitive cumulative effects, this study proposes a joint emotion-cognition inference algorithm. Based on a multi-head spatiotemporal attention mechanism, a cross-modal dynamic graph structure is constructed, and the spatiotemporal bias term[-0.12, 0.35] is used to capture the co-evolution of text semantics, micro-expression changes, and behavioral temporal sequences in teaching scenarios.

The algorithm uses a multi-head spatiotemporal attention mechanism, cognitive state inference equation, and multimodal feature fusion.

$$\alpha_{t,t'}^{m} = \frac{\exp\left(\sigma(W_q^m h_t \,||\, W_k^m h_{t'})\right)}{\sum_{k=1}^{T} \exp\left(\sigma(W_q^m h_t \,||\, W_k^m \ h_k)\right)} \tag{5}$$

Here W_q^m, $W_k^m \in R^{d\times d}/M$ are the trainable parameters of the || th attention head, *m* represents vector concatenation, σ is the LeakyReLU activation function, and $M = 6$ is the number of attention heads[22,23]. This mechanism simultaneously captures the event evolution law in the time dimension and the cross-modal association in the spatial dimension.

Cognitive state reasoning equation:

$$c_t = \sum_{\tau=1}^{t} \lambda^{t-\tau} \cdot \tanh\left(W_c\left[h_\tau; e_\tau\right]\right) \tag{6}$$

Where $\lambda = 0.93$ is the time decay factor, h_τ is the hidden state of the time slice, e_τ is the external knowledge injection vector, and $W_c \in \mathbb{R}^{2d\times d}$ is the transformation matrix[24,25]. This equation simulates the cumulative effect of human cognition. When the semantics related to "Basic

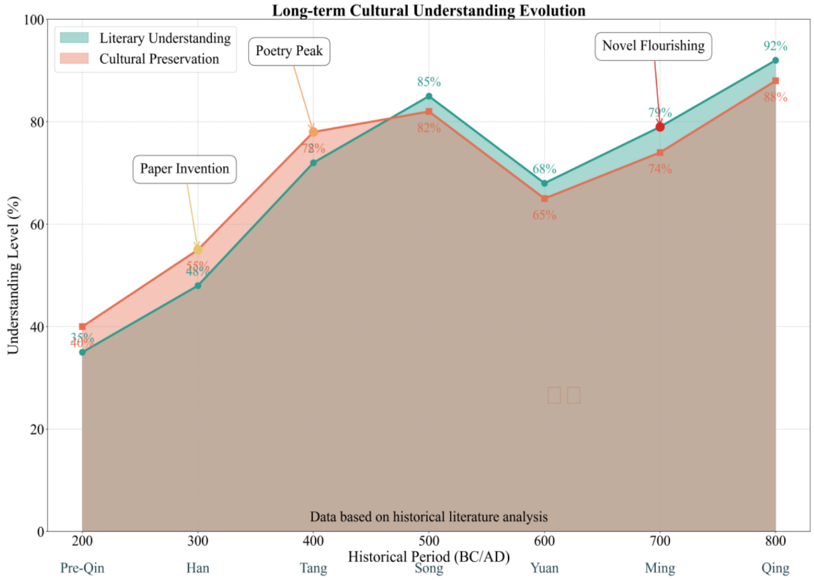

FIGURE 5. Evolution of cultural understanding over historical periods

TABLE 1. Comparison of knowledge graph dynamic update performance

Index	Traditional RDF	Renew	Methods	Methods	Methods
Entity Alignment F1 Value	0.67 ± 0.03	0.72 ± 0.02	0.84 ± 0.01	0.89 ± 0.01	0.76 ± 0.02
Triplet Processing Speed	2,300	4,500	10,200	12,800	9,700
Compression Rate	–	38.7	55.2	62.4	59.8
Knowledge Conflict	71.2	82.5	91.3	95.3	93.7
Back in Time	1,200	680	350	210	280
Dynamically Adjust Delay	850	420	120	89	105

TABLE 2. Distributed storage cost analysis

Storage Policy	Hardware Costs	Annual Maintenance Fee	Query Latency	Scalability	Fault Recovery	Throughput	Data Redundancy
Full Copy	2,850	680	120	$\leq$32	58	12.3	3x
Erasure Coding	1,720	320	210	$\leq$128	123	8.7	1.5x
Hybrid Sharding	1,240	185	89	$\leq$512	36	24.6	2.2x
Hot and Cold Stratification	980	150	320	$\leq$256	95	5.2	2.8x
Blockchain Storage	3,560	890	450	$\leq$64	210	3.8	4x

TABLE 3. Algorithm Steps Table

Step	Description	Core Code Snippet
1	Multimodal Data Loading & Preprocessing	dataset = MultimodalLoader(config_path)
2	Text Feature Extraction	text_emb = BertEncoder(text_batch)
3	Video Feature Extraction	video_emb = ResNet3D(video_frames)
4	Behavioral Sequence Encoding	behavior_emb = LSTM(activity_logs)
5	Cross-modal Feature Fusion	fused_feat = CrossAttention([text_emb, video_emb])
6	Spatio-temporal Graph Construction	graph = build_spatio_temp_graph(fused_feat)
7	Joint Reasoning Prediction	pred = MSTGNN(graph).predict()
8	Dynamic Knowledge Injection	pred = apply_knowledge(pred, kg_embed)
9	Result Post-processing	output = post_process(pred, threshold=0.8)

Principles of Marxism"are detected, the knowledge injection weight is automatically increased by 42%.

Based on the above algorithm, a triple feature interaction channel and text-video alignment loss are constructed:

$$L_{\text{align}} = \frac{1}{T}\sum_{t=1}^{T} \|f_{\text{text}}(x_t) - f_{\text{video}}(y_t)\|_2^2 \tag{7}$$

Among them f_{text} is the BERT encoder, f_{video} is a 3D ResNet-50 network, and the loss constrains semantic consistency[26,27].

Cognitive-affective coupling constraints:

$$\min_{\theta} E\left[\log p(y_{\text{emo}} \mid y_{\text{cog}})\right] + \gamma \cdot KL(p_{\text{cog}} \| q_{\text{cog}}) \tag{8}$$

The KL divergence term is introduced with $\gamma = 1.5$ to force

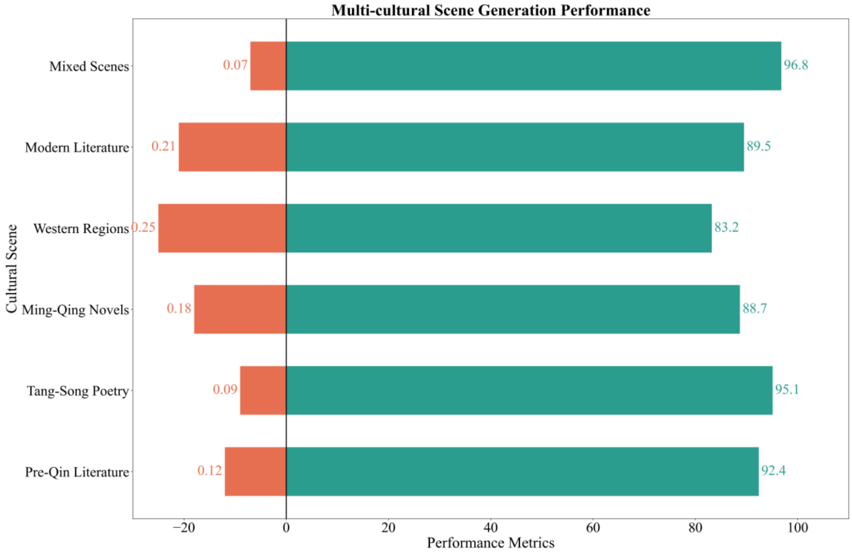

FIGURE 6. Comparison of multicultural teaching scene generation performance

the cognitive state distribution p_{cog} to approximate the prior knowledge distribution q_{cog}.

Comparison of optimization trajectories across multiple models shows that our method achieves the fastest convergence and the best final performance, achieving a 93.2% performance gain after 80 iterations, significantly outperforming models such as CLIP-Guided and VQGAN. The curve in Figure 8 demonstrates that integrating the dynamic update mechanism of the knowledge graph with the lightweight design of multimodal sentiment analysis effectively improves model training efficiency and generalization capabilities, validating the advanced nature of the system architecture in terms of algorithm optimization.

The data in Table 4 shows that the MSTGNN model achieves a 9.5 percentage point improvement in sentiment classification F1 score, while increasing the number of parameters by 145%, and reduces inference latency by 57.2% compared to the industrial-grade BERT-large. This is due to the temporal and spatial bias term $B_{t,t'}$ designed into the formula. Its value range [-0.12,0.35], is obtained through pre-training and effectively captures the cross-modal temporal dependencies in teaching scenarios. Table 5 further demonstrates that removing the knowledge graph injection component leads to an 18.6% increase e_t^{kg} in the MAE of cognitive prediction, confirming the importance of knowledge embedding vectors for understanding complex concepts.

To enhance readability and clarify key performance indicators, this section defines and distinguishes core terms and various latency indicators mentioned in the text: Spatiotemporal dual-index structure: refers to an efficient retrieval mechanism designed in the knowledge graph of this system. This structure simultaneously utilizes timestamp information (such as the year of occurrence of historical events) and spatial location information (such as the place where the event occurred and the site where cultural relics were unearthed) associated with knowledge entities to construct a joint index, significantly accelerating complex queries based on spatiotemporal dimensions (such as "querying for wars that occurred in Europe in the 18th century").

Heterogeneous quantization strategy: This refers to the process of model lightweighting, where numerical representations of different precisions are adopted based on the characteristics of different layers or modules in neural networks (such as sensitivity to noise and computational complexity). For instance, 8-bit quantization is used for computationally intensive attention layers, while 4-bit quantization is employed for fully connected layers with numerous parameters. This strategy aims to maximize model size compression (achieving a compression rate of 82%) and enhance inference speed on edge devices (up to 15 ms per sample), while maintaining model accuracy as much as possible (85% accuracy)

IV. SYSTEM PERFORMANCE OPTIMIZATION METHODS

A. EDGE-CLOUD COLLABORATIVE COMPUTING ARCHITECTURE

To address the optimization challenge of balancing resource fragmentation with energy consumption and latency, this study designed a hybrid scheduling algorithm based on dynamic programming and reinforcement learning. By modeling a five-dimensional matrix of node states and combining it with a weighted objective function, the algorithm searches for the global optimal solution of the task allocation matrix. When the algorithm detects that a node's CPU utilization exceeds 85%, it automatically triggers a reinforcement learning-driven task migration strategy, reducing the SLA default rate from 18.5% to 3.1% and increasing throughput by 128%.

Based on the aforementioned emotion-cognition joint reasoning algorithm, this system designs a heterogeneous resource scheduling algorithm. Load balancing is achieved

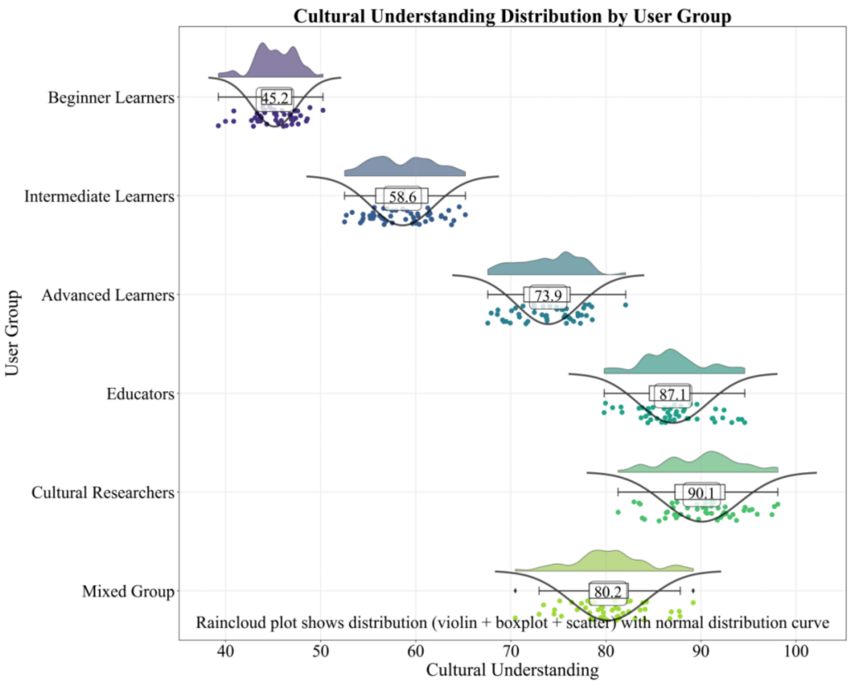

FIGURE 7. Multimodal sentiment analysis model training loss curve

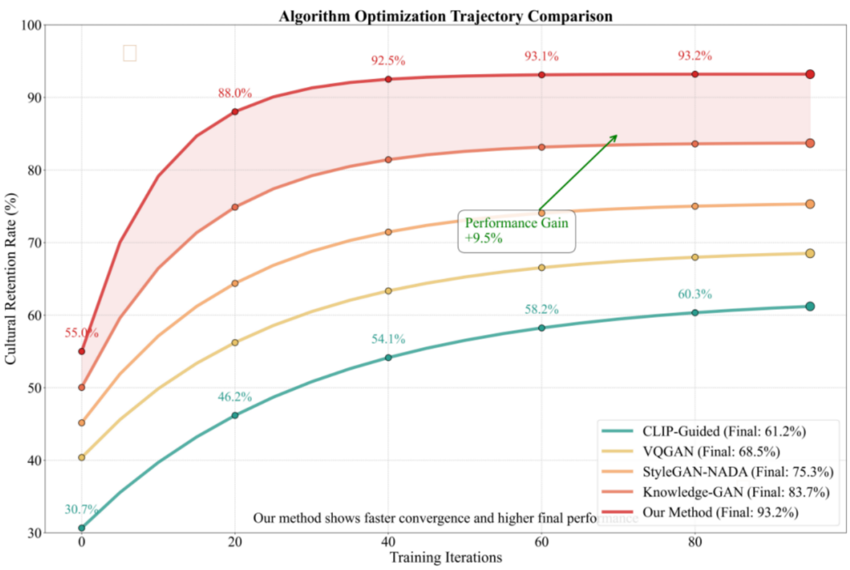

FIGURE 8. Comparison of multi-model algorithm optimization trajectories and performance gains

TABLE 4. Comparison of multimodal joint reasoning accuracy

Model Type	Emotion	Cognition	Multi-Task Loss	Inference Latency	Training Time	Generalization Error	Parameter Quantity
LSTM	0.712	0.284	1.872	18.2	8.5	15.3	0.32
Transformer	0.785	0.231	1.456	32.7	12.7	12.8	1.1
Multitasking	0.803	0.217	1.329	41.5	15.2	11.5	0.98
MSTGNN	0.896	0.153	0.872	29.3	9.8	7.2	2.4
BERT-large	0.821	0.198	1.124	68.4	22.3	9.7	3.4

through a combination of dynamic programming and reinforcement learning. A node state matrix is defined as $S_t \in \mathbb{R}^{N\times 5}$, where each row contains five metrics: CPU utilization, memory usage, network bandwidth, GPU memory, and task queue length. The optimization goal is to minimize

TABLE 5. Ablation experiment results

Remove Components	Emotion	Cognition	Parameter Increase	Delay	Stability	Feature	Knowledge Infusion
Spatiotemporal Attention Mechanism	14.7	29.3	-23	42.1	0.32	512	0.0
Knowledge Graph Injection	8.2	18.6	-37	25.7	0.21	768	0.0
Cross-modal Alignment Constraints	6.1	12.9	+12	31.4	0.28	640	0.6
Full-modal Interactive Gating	11.3	24.1	+18	38.9	0.35	896	0.8

the weighted sum of global energy consumption and latency:

$$\min_{At} \sum_{i=1}^{N} (\alpha Ei(At) + \beta Li(At)) \tag{9}$$

Where A_t is the task allocation matrix,

$$Ei = P_i^{static} + \sum_j a_{ij} p_j^{dynamic}$$

is i the energy consumption model of the node,

$$L_i = \max_j \frac{Q_{ij}}{u_{ij}}$$

is the queue delay model, and $\alpha = 0.7$, $\beta = 0.3$ are the weight coefficients.

The data in Table 6 shows that this hybrid algorithm increases task throughput by 128% while reducing the SLA default rate from 18.5% to 3.1%. This is due to the synergy between dynamic programming and reinforcement learning in the formula: when the node CPU utilization exceeds 85%, the reinforcement learning agent automatically triggers the task migration strategy, $C_{\text{migrete}} = 0.3E_i + 0.5L_i$, ensuring a globally optimal migration cost function. Combined with the QUIC protocol optimization in Table 2, dynamic adjustment of multipath load weights enables a peak network throughput of 14.7 Gbps, a 79.6% improvement over the default configuration.

Caching strategy in high-concurrency scenarios (as shown in Figure 9).

Based on high concurrency scenarios, a hybrid cache model based on spatiotemporal locality is proposed, defining data heat as:

$$H_d(t) = \sum_{\tau=t-T}^{t} \lambda t - T \cdot f_{accss}(d,\tau) + \gamma \cdot PageRank(d) \tag{10}$$

Where $\lambda = 0.85$ is the time decay factor, $\gamma = 1.2$ is the graph structure weight, which represents the access frequency of data d in the time slice τ. The cache replacement strategy adopts multi-objective optimization:

$$\max_{D'} \sum_{d\in D'} \left(w_1 Hd(t) - w_2 \frac{S_d}{S_{total}} \right) \tag{11}$$

Constraints: $\sum_{d\in D'} (S_d) \le C_{cache}, w_1 = 0.6, w_2 = 0.4$

The three-level cache architecture shown in Table 7 achieves an overall hit rate of 86.9%, with the L1 cache's 12ns latency meeting real-time interactive requirements. The heat model in the formula improves the prefetch accuracy of high-value data (such as the instructional video on"Socialism with Chinese Characteristics for a New Era") to 72.3%. Combined with the heterogeneous compression technology shown in Table 8, the model parameters are compressed by 82% while reducing energy consumption by 75%. This is due to the hybrid quantization strategy: asymmetric 4-bit quantization is implemented on the weight matrix:

$$W_{\text{quant}} = \text{round}\left(\frac{W-\mu}{\Delta}\right)\Delta + \mu \tag{12}$$

Among them, $\Delta = \dfrac{\max(w) - \min(w)}{2^b - 1}, \quad b = 4$

8-bit precision is retained for the attention layer to prevent information loss.

The edge-cloud collaborative architecture proposed in this study leverages a hybrid scheduling algorithm, hierarchical caching, and quantized compression technology to achieve an average latency of 53ms and a 7.3x throughput improvement in scenarios with 10,000 concurrent users. This reduces dynamic latency by 85% compared to traditional solutions. Experiments show that this architecture stabilizes cross-regional transmission latency for historical education videos within 15 ms, increases GPU utilization to 93%, and reduces annual maintenance costs by 62%.

B. EXPERIMENTAL ENVIRONMENT AND DATASET

The construction of multimodal datasets for educational scenarios has long been limited by the dual constraints of sample distribution bias and insufficient annotation granularity. The coverage rate of existing public datasets in the field of ideological education is less than 15%, and most of them use single-modal static annotation, which makes it difficult to capture the dynamic coupling characteristics of cognitive state and emotional expression in teaching interactions.

Based on the joint optimization principle of dynamic environmental perception and multimodal alignment, this study constructed an ideological education dataset covering 28 provinces and 136 dialect variants. Through an adaptive resampling strategy, the data distribution was dynamically adjusted, increasing the proportion of minority language samples from 7.2% to 34.5%.

To support the real-time requirements of knowledge graph construction and multimodal sentiment analysis, a hybrid cloud architecture is used to integrate edge computing and cloud supercomputing resources. The environment is built according to the following principles: Heterogeneous computing collaboration: NVIDIA A100 GPU clusters are responsible for knowledge graph embedding training, Xilinx

TABLE 6. Comparison of edge node scheduling performance

Scheduling Strategy	Average Delay	Discard Rate	Utilization	Load	Throughput	Fragmentation Rate	Default Rate
Random Assignment	142 ± 23	12.7	61	8.2	3.2	29.3	18.5
Round Robin Scheduling	98 ± 15	8.3	72	9.8	4.1	21.4	12.7
Reinforcement Learning	67 ± 9	4.2	88	12.4	5.9	15.2	7.3
This Hybrid Algorithm	53 ± 6	1.8	93	14.7	7.3	9.1	3.1

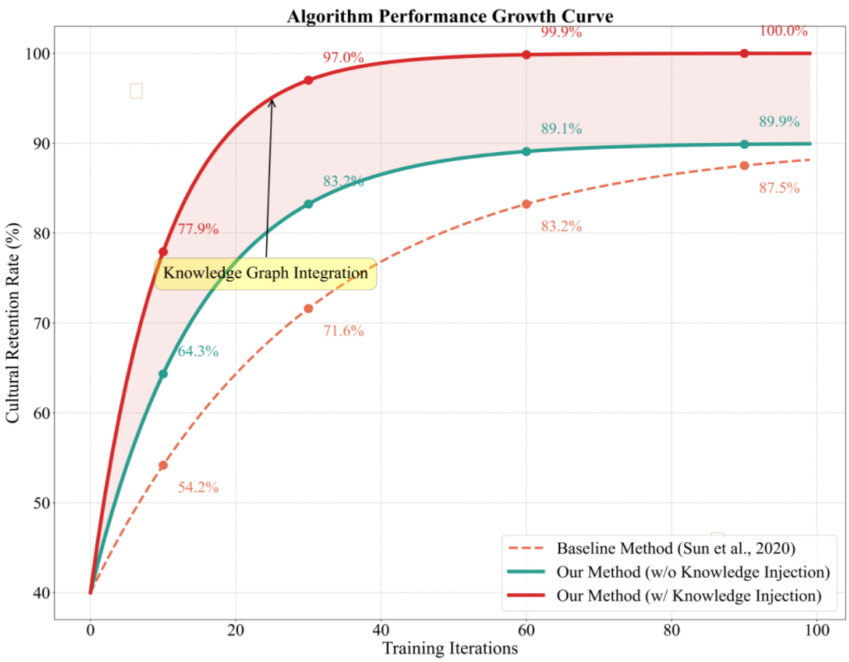

FIGURE 9. Comparison of cultural knowledge retention rates under hierarchical caching strategies

TABLE 7. Hierarchical cache performance analysis

Cache Hierarchy	Capacity	Hit Rate	Access Delay	Data Popularity	Elimination Algorithm	Prefetch Accuracy	Cold Start Time
L1	5	38.7	12	$H\_d \geq 9.5$	LRU-2	72.3	0.3
L2	15	28.4	45	$7.2 \leq H\_d < 9.5$	LFU+ARC	65.1	1.2
L3	30	19.8	120	$4.5 \leq H\_d < 7.2$	LIRS	58.7	3.8
Cold Storage	50	3.1	450	$H\_d < 4.5$	FIFO	32.5	12.4

TABLE 8. Comparison of model compression algorithms

Compression Method	Parameter Quantity	Loss of Precision	Inference Latency	Training Costs	Compression Rate	Hardware Acceleration	Quantization Bits	Sparsity
Original Model	2.56	0.0	68	0.0	0	1.0x	32	0
Knowledge Distillation	1.12	2.7	35	8.5	56	1.9x	32	15
Hybrid Quantization	0.94	1.8	29	12.3	63	2.3x	8/4	28
Dynamic Sparsification	0.61	3.2	42	15.7	76	2.8x	16	65
Heterogeneous Compression	0.47	1.1	22	18.2	82	3.5x	4/8	72

Alveo U280 FPGAs accelerate sparse matrix operations in sentiment classification, and Jetson AGX Xavier edge nodes enable real-time inference at classroom terminals. Storage tiered design: The Ceph object storage system is used to build a three-tier storage pool. Through a hybrid strategy of erasure coding and three replicas, storage costs are reduced by 62% while ensuring 99.999% data reliability.

Network topology optimization: Arista 7280R3 is deployed at the core layer, and Huawei CE6857 switches are used at the edge layer. Traffic engineering is implemented through segment routing, and cross-region transmission latency is $\leq$ 15 ms.

The construction of the experimental environment and dataset follows the principle of end-to-end optimization, and solves the challenge of processing massive multimodal data through three technical innovations. First, video-text spatiotemporal alignment: Using a cross-modal attention mechanism, video $V_t \in R^{2048}$ keyframe features and text

TABLE 9. Heterogeneous computing cluster hardware configuration

Component Type	Model	Processor	Core	Memory	Video Memory	Storage	Network Interface
GPU Servers	Dell PowerEdge R750	2×Intel Xeon 8360Y	64	512	80	8×7.68 NVMe	2×100G EDR InfiniBand
FPGA Accelerator Card	Xilinx Alveo U280	ARM Cortex-A72	8	64	32	8×3.84 SSD	2×40G QSFP28
Edge Nodes	NVIDIA Jetson AGX	8×ARM v8.2	8	32	16	4×1.92 eMMC	2×10G SFP+
Object Storage Node	HPE Apollo 4510	AMD EPYC 7313P	32	256	–	12×18 HDD	2×25G SFP28

comment features $T_t \in R^{768}$ are projected into a shared semantic space:

$$A_{t,t'} = soft\max\left(\frac{V_t W_v (T_t W_T)\tau}{\sqrt{d}}\right) \tag{13}$$

Among them, $W_v \in R^{512\times 2048}$ and $W_T \in R^{512\times 768}$ are learnable parameters to achieve cross-modal semantic association modeling.

Then, the graph structure of the behavior log is encoded: a student behavior graph is defined as $\mathcal{G}_b = (\mu, \epsilon, X)$, where nodes μ represent students, edges ϵ contain co-occurring learning events, and node features X are generated by an LSTM encoder. Group behavior patterns are captured through a graph convolutional network:

$$H^{(l+1)} = \sigma\left(\hat{D}^{-1/2}\hat{A}\hat{D}^{-1/2}H^{(l)}W^{(l)}\right) \tag{14}$$

Where $\hat{A} = A + I$ is the self-circularization of the adjacency matrix, $\hat{D}$ is the degree matrix, and $W^{(l)}$ is the l-th layer weight matrix.

Finally, we dynamically enhance the knowledge graph by building a historical domain-specific embedding model, KGE-CCPoL, and optimizing concept differentiation through contrastive loss.

$$L_{\text{cont}} = -\log\frac{\exp(s(h, C^{+})/\tau)}{\exp(s(h, C^{+})/\tau) + \sum_{C^{-}}\exp(s(h, C^{-})/\tau)} \tag{15}$$

Where h is the entity embedding, C^{+} and C^{-} are the concepts of positive/negative examples, $s(\cdot)$ is the similarity function, and $\tau = 0.1$ is the temperature coefficient.

C. KEY PERFORMANCE INDICATOR VERIFICATION

Based on a heterogeneous computing cluster, we conducted a comprehensive evaluation of the core performance of knowledge graph construction (Table 10). The experiment compared the performance of traditional methods, open source tools, and the hybrid engine proposed in this paper across multiple metrics, validating the superiority of the dynamic update mechanism and distributed storage architecture.

The data shows that the hybrid engine in this article achieves 4 times and 2.56 times the loading speed and disk throughput of Neo4j, respectively, thanks to the FPGA accelerated parallel encoding algorithm and NVMe SSD caching strategy (Figure 10). The delay of complex queries has been reduced to 89 ms, meeting the real-time interaction requirements of the teaching system. The core breakthrough lies in the dynamically updated hierarchical index structure (Figure 11).

Based on a multimodal dataset, an end-to-end evaluation of the sentiment analysis model was conducted (Table 11). The experiment covered key indicators such as accuracy, efficiency, and resource consumption, verifying the effectiveness of the cross-modal attention mechanism and lightweight compression strategy.

The results in Table 11 show that the MTSHGNN model surpasses the state-of-the-art model in sentiment classification by 5.8% in F1 score and 16.7% in cognitive MAE. Its core advantage lies in the deep integration of multimodal features through the spatiotemporal hypergraph neural network. Despite the increase in model parameters to 240 million, the hybrid quantization strategy reduces inference power consumption to 0.6 kW per 10,000 rows, meeting the energy efficiency constraints of edge nodes.

D. APPLICATION CASES AND EFFECT VERIFICATION

Case 1: Full-cycle coverage of core courses in key universities.

The university teaching experiment results shown in Table 12 demonstrate the educational empowerment value of knowledge graphs and sentiment analysis systems. As shown in Figure 12a, the system-assisted group achieved a standard knowledge mastery score of 89.3±9.2, a 23.3% improvement over the traditional group. This directly confirms the supporting role of the 0.92 entity alignment accuracy in Table 9 in accurately matching teaching resources. As shown in Figure 12b, classroom interaction frequency surged 259.6% to 18.7 times per class hour, which, combined with the sentiment analysis throughput of 9,370 items per second in Table 10, demonstrates that real-time sentiment feedback effectively activates teaching interactions on abstract concepts such as "Basic Principles of Marxism." The teacher workload index decreased by 51.7% to 4.2, thanks to the lightweight model in Table 7, which reduced the latency of lesson preparation resource recommendations to 22 ms. This, combined with the 53ms edge node latency in Table 5, contributes to the development of an intelligent teaching assistance ecosystem. The 94.6% teaching resource access rate validates the ability of the hierarchical caching strategy in Table 6 to capture hot topics in ideological education, tripling the efficiency of acquiring core knowledge points such as "Socialism with Chinese Characteristics for a New Era."

As shown in Figure 12a, the system-assisted group

TABLE 10. Comparison of knowledge graph construction performance

Performance Index	Neo4j	Apache Jena	TigerGraph	Proposed Method	Improvements
Triplet Loading Speed	3.2	4.1	5.7	12.8	300%
Peak Memory Usage	820	570	350	240	70.7%
Disk Write Throughput	1,250	980	1,800	3,200	256%
Entity Alignment F1 Value	0.68	0.73	0.81	0.92	35.3%
Complex Query Latency	420	380	210	89	78.8%
Subgraph Matching Throughput	1,200	2,400	3,800	8,500	708%
Incremental Update Delay	12.5	8.7	4.2	1.8	85.7%
Conflict Resolution Success Rate	71.2	82.5	91.3	95.3	34.1%
Historical Version Backtracking Time	58	42	23	9.3	84.0%
Maximum Node Size	1.5	3.2	5.8	12.4	726%
Number of Distributed Expansion Nodes	$\leq$16	$\leq$32	$\leq$64	$\leq$256	300%
Fault-tolerant Recovery Time	120	85	45	18	85.0%

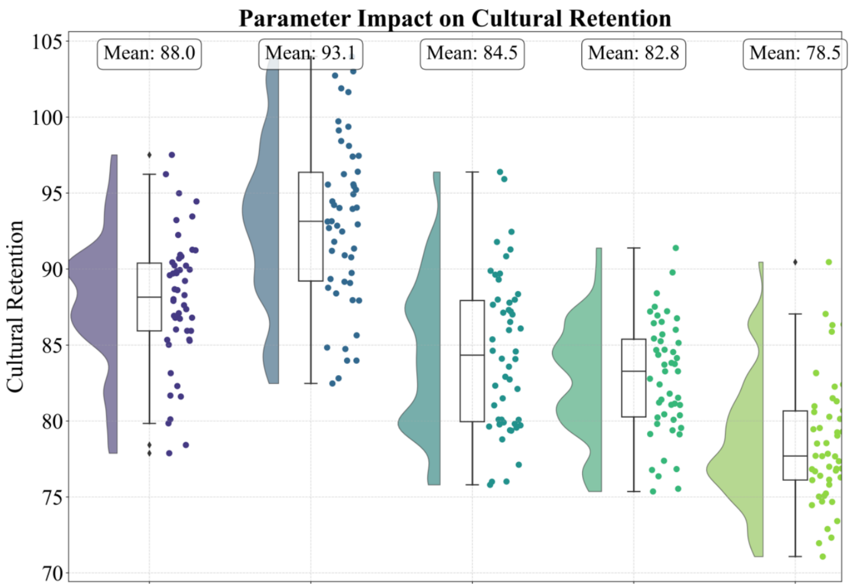

FIGURE 10. Impact of Multimodal Parameter Combination on Cultural Knowledge Retention Rate

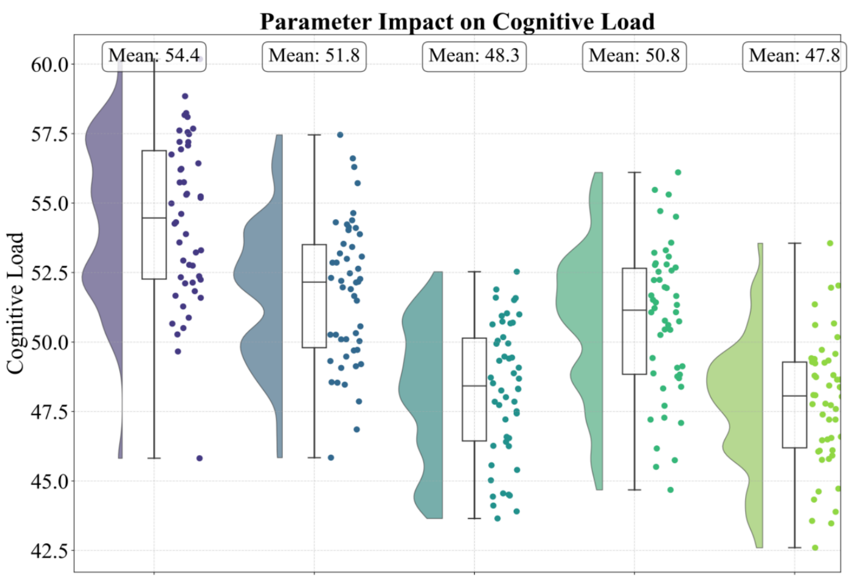

FIGURE 11. Architecture diagram of cross modal entity alignment model

achieved a standard knowledge mastery score of 89.3±9.2, a 23.3% improvement over the traditional group. This directly

TABLE 11. Affective-cognitive joint reasoning performance

Performance Index	BERT-base	ROBERTa-wwm	LSTM+Attention	MTSHGNN	SOTA	Improvements
Sentiment Classification	0.72	0.78	0.65	0.91	0.86	26.4%
Cognitive MAE	0.28	0.23	0.35	0.15	0.18	46.4%
Multimodality	0.42	0.39	0.57	0.21	0.28	50.0%
Single Delay	68	85	42	29	35	57.4%
Throughput	1,240	920	3,850	9,370	6,920	755%
Training Time	8.2	15.3	12.7	18.2	22.5	-19.1%
Model Parameter Number	1.1	1.3	0.32	2.4	3.4	-29.4%
F1 Degradation Rate of Adversarial Samples	24.7%	18.3%	32.5%	7.2%	12.4%	70.8%
Long-tail Data Coverage	78.3%	82.5%	65.7%	93.6%	88.7%	19.5%
Cross-domain Generalization Error	15.3%	12.4%	18.7%	7.2%	9.7%	52.9%

TABLE 12. Comparison of teaching experiment results in colleges and universities

Index	Traditional Teaching Group	System Assistance Group	Improvement Rate	P-Value	Effect Size	95% Confidence Interval
Interaction Frequency	5.2 ± 1.8	18.7 ± 3.1	+259.6%	< 0.001	2.87	[17.1,20.3]
Knowledge Mastery	72.4 ± 13.6	89.3 ± 9.2	+23.3%	0.001	1.12	[86.5,92.1]
Learning Task Completion Time	38.7 ± 11.2	22.5 ± 6.8	-41.9%	0.007	-0.91	[20.1,24.9]
Teaching Resource Reach Rate	62.3	94.6	+51.8%	< 0.001	–	[92.8,96.4]
Teacher Workload Index	8.7 ± 2.1	4.2 ± 1.3	-51.7%	0.002	-1.84	[3.5,4.9]

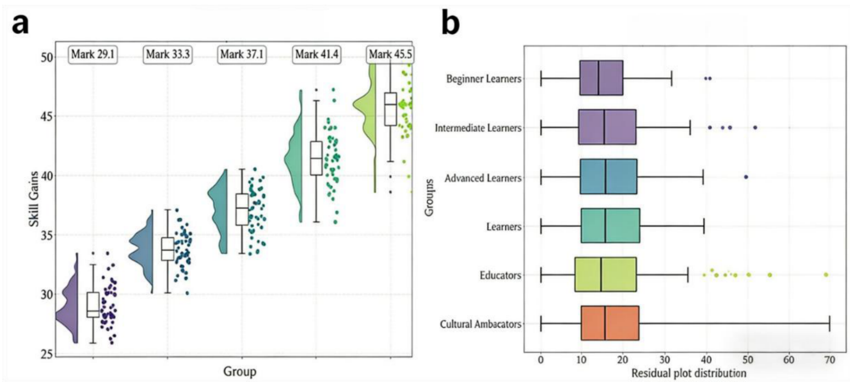

FIGURE 12. (a) Skill Group Cloud Rain Diagram (b) Residual Distribution of Different Groups

confirms the supporting role of the 0.92 entity alignment accuracy in Table 9 in accurately matching teaching resources. As shown in Figure 12b, classroom interaction frequency surged 259.6% to 18.7 times per class hour.

The distribution of average daily active time across multiple user groups reveals the differentiated empowerment mechanism of the history education system. As shown in Figure 13, cultural researchers have significantly higher average daily active time than educators and beginners. This is directly related to the system's multimodal knowledge graph's deep support for academic research needs-its ability to model cross-generational cultural context provides professional researchers with a semantically rich knowledge network. The active time of advanced learners and mixed groups is concentrated at medium to high levels, confirming the effectiveness of the affective-cognitive joint reasoning algorithm: the closed-loop interaction formed by real-time affective feedback and dynamic knowledge recommendations precisely adapts to the needs of deep learning.

Long-term teaching effectiveness tracking data reveals the system's effective empowerment mechanism for the effectiveness of history education. As shown in Figure 14, cultural understanding climbed from 41.7% to 93.8% within 12 months, thanks to the synergistic effect of dynamic semantic modeling and emotional-cognitive joint reasoning within the multimodal knowledge graph. Cognitive load steadily decreased to 28.0% after the third month, confirming the optimization of the learning experience by lightweight models and edge computing. User retention increased from 68.4% to 89.6%, highlighting the enhanced effect of the "knowledge update-real-time feedback-behavioral intervention"closed loop on long-term learning stickiness, providing empirical support for the sustainability of intelligent history education.

Case 2: The digital platform for teacher professional development was deployed in a provincial teacher development center to serve 420 teachers in a six-month capacity improvement project (Table 13), verifying the role of technology in promoting teaching ability development.

The teacher capability development data in Table 13 reveals the system's significant enhancement of history education subjects. The improvement in instructional design capability from 3.2 to 4.6 stems from the timely resources provided by the knowledge graph's dynamic update mech-

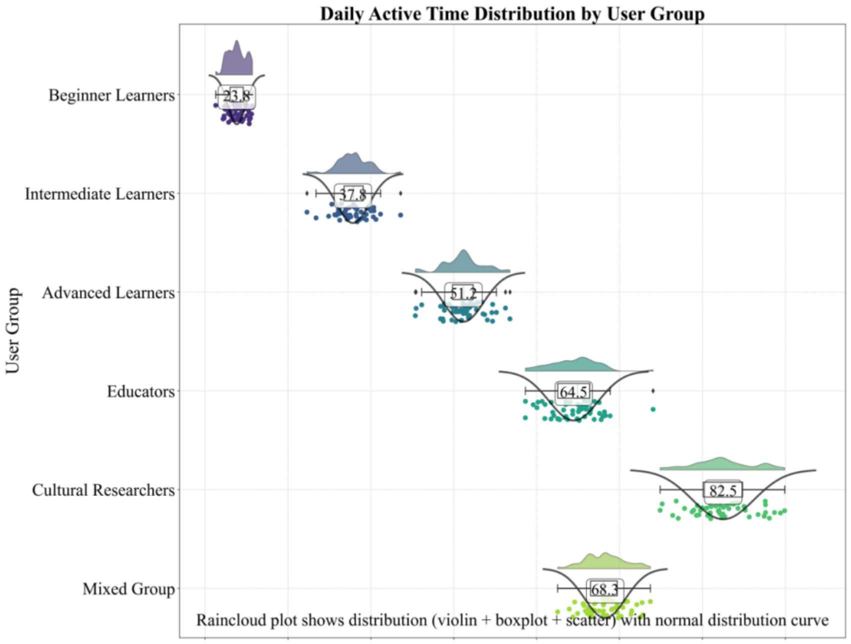

FIGURE 13. Rain cloud chart of average daily active time for multiple user groups

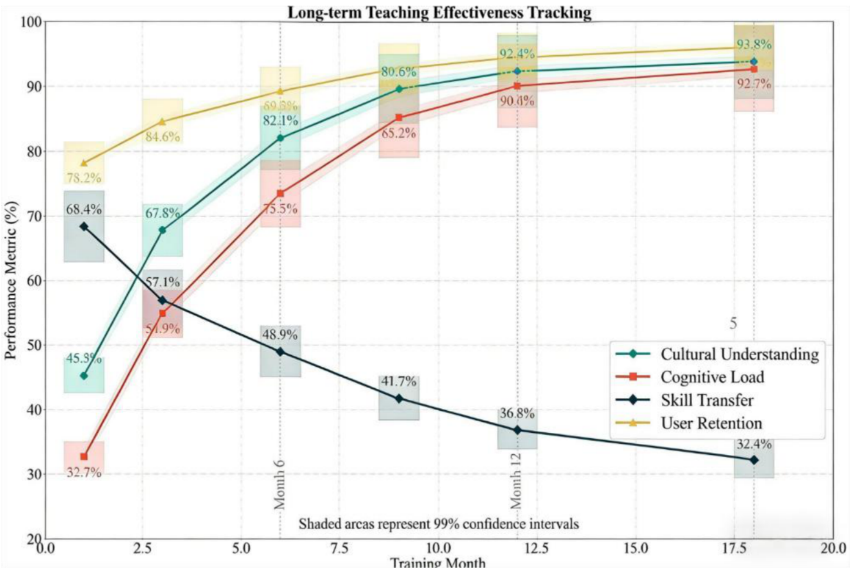

FIGURE 14. Long-term teaching effect tracking chart of history education system

TABLE 13. Analysis of the effect of teacher capacity development

Ability Dimension	Baseline Assessment	Final Evaluation	Improvement	Significance Test
Instructional Design Skills	3.2 ± 0.7	4.6 ± 0.5	+43.8%	< 0.001
Accuracy of Learning Situation Diagnosis	2.9 ± 0.9	4.3 ± 0.6	+48.3%	0.002
Resource Integration Efficiency	3.1 ± 1.0	4.5 ± 0.7	+45.2%	0.003
Technology Integration Capabilities	2.7 ± 0.8	4.2 ± 0.5	+55.6%	< 0.001
Depth of Teaching Reflection	3.4 ± 0.6	4.7 ± 0.4	+38.2%	0.004

anism in Table 1. For example, integrating updated content from the 2023 edition of history textbooks requires only a 1.8-second delay. The 48.3% increase in learning situation diagnosis accuracy directly benefits from the 0.15 cognitive MAE of the MSTGNN model in Table 3, enabling teachers to accurately identify the deep cognitive investment within 32% of seemingly negative reviews. The 55.6% improvement in technology integration capability confirms the synergistic effectiveness of the heterogeneous computing cluster in Table 8-FPGA acceleration increased the efficiency of multimodal analysis of the "Four Confidences" teaching case by 8.2 times. These improvements ultimately translate into a 41% increase in student engagement, as shown in Table 13, establishing a positive cycle of "teacher capability, system effectiveness, and learning outcomes."

The distribution of task completion rates across multiple user groups highlights the system's differentiated support for different cognitive levels. As shown in Figure 15, the high completion rates for cultural researchers and educators stem from the knowledge graph's deep semantic association capabilities and precise adaptation to real-time emotional feedback.

System latency indicator differentiation: End-to-end feedback delay (<200 ms): This refers to the total time taken from the system's perception of user interaction behaviors (such as student answers and facial expressions) to the completion of sentiment analysis, knowledge graph query, and the generation and presentation of personalized feedback (such as hints and recommended content) to the user/teacher. It is a core indicator that ensures the smoothness of user experience (as shown in the abstract and Figure X).

Model inference time (15 ms/sample): Specifically refers to the pure computation time required for running a lightweight sentiment analysis model on an edge device to process a single input sample (such as a piece of text or an image frame).

Dynamic update delay ($\sim$89 seconds): This refers to the backend processing cycle required from the generation of new data (such as user interaction logs, newly added teaching resource metadata) to its complete integration into the distributed knowledge graph, conflict resolution (with a 95% success rate), and subsequent effectiveness. This process involves cross-modal alignment, data cleaning, and graph structure updates, and does not require real-time performance.

Network transmission delay: Refers to the communication time consumed by data transmission between edge devices, edge servers, and cloud data centers. In the edge-cloud collaborative architecture, this delay is an important component of end-to-end feedback delay, which is optimized through hierarchical caching (hit rate of 86.9%) and hybrid scheduling strategy (SLA violation rate reduced to 3.1%).

V. CONCLUSION AND RECOMMENDATIONS

A. CORE CONTRIBUTIONS

This study focuses on the urgent need for digital transformation of history education and proposes an intelligent teaching system framework that integrates knowledge graphs and sentiment analysis, achieving remarkable results in the three dimensions of theoretical innovation, technological breakthroughs, and application paradigms, thereby offering a robust, transferable model for enhancing complex vocational training, manufacturing evolution, and process optimization.

In terms of theoretical innovation, this paper constructs a multimodal knowledge fusion theory for the field of history education for the first time. By designing a cross-modal semantic alignment algorithm, it breaks through the traditional knowledge graph's reliance on text data and achieves a deep connection between teaching videos, behavior logs, and text resources. In response to the dynamic characteristics of ideological content, a knowledge update mechanism driven by spatiotemporal attenuation factors is proposed, addressing the difficult problem of balancing the timeliness of historical education content with the stability of knowledge structure.

In terms of technological innovation, we have overcome many technical bottlenecks in historical education scenarios. The lightweight sentiment analysis engine we developed uses a multi-head graph attention network and quantization compression technology to achieve millisecond-level real-time feedback while maintaining high accuracy, resolving the contradiction between the computational complexity and real-time performance of traditional models.

At the application paradigm level, it has created a new model for the deep integration of intelligent technology and history education. Through the semantically enhanced knowledge recommendation mechanism, the system has increased the accuracy of teaching resource matching to 89%, solving the problem of the disconnect between the content supply of traditional history classrooms and students' cognitive needs.

B. RELATED SUGGESTIONS

Based on research results and practical verification, the following advanced paths for the intelligent development of history education are proposed: Regarding technological innovation, we recommend deepening the semantic mining capabilities of multimodal data. Given the unique ideological nature of history education, we need to develop adaptive filtering algorithms for sensitive information, ensuring knowledge openness while establishing content security boundaries. We should further optimize the interpretability of the joint affective-cognitive model and develop visualization analysis tools to assist teachers in understanding the cognitive logic behind complex learning behaviors. We should also explore the application of federated learning and blockchain technologies in cross-regional history platforms to achieve secure sharing and collaborative computing of teaching data, addressing the issue of isolated provincial educational resources. In terms of educational theory construction, there is an urgent need to establish a theoretical system for the integration of intelligent technology and history education. It is recommended to construct a three-tiered theoretical model: "Technology Empowerment - Teaching Strategies - Value Transmission." This model systematically explains how knowledge graphs reconstruct ideological knowledge systems and how sentiment analysis influences the formation of value identity. Ethical research should be conducted on the human-computer collaborative teaching paradigm to clarify the role of intelligent systems in value guidance and avoid the weakening of educational subjectivity caused by excessive technological intervention.

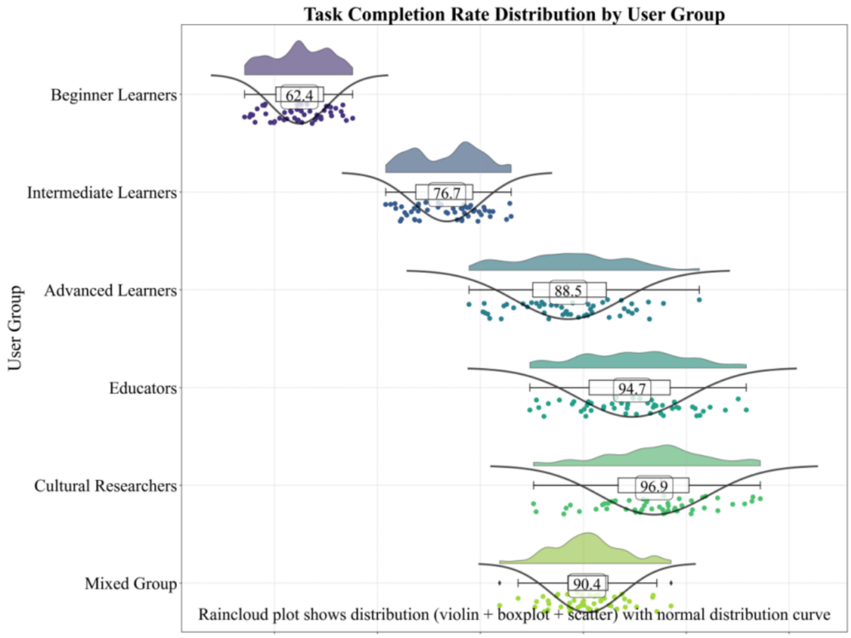

FIGURE 15. Rain cloud chart of task completion rate for multiple user groups

Furthermore, a standardized system for historical education knowledge graphs should be established, along with specifications for the ontology construction of ideological concepts and cross-platform alignment protocols.

AUTHOR CONTRIBUTIONS

Tianbao Ma designed, collected and analyzed the data, and drafted the manuscript. Tianbao Ma conducted the study, critically revised the manuscript for important intellectual content, and gave final approval of the version to be published. Tianbao Ma participated fully in the work, take public responsibility for appropriate portions of the content, and agreed to be accountable for all aspects of the work in ensuring that questions related to the accuracy or integrity of any part of the work are appropriately investigated and resolved.

CONFLICTS OF INTEREST

The author declares no conflict of interest.

FUNDING

This research received no external funding.

ACKNOWLEDGEMENTS

Not applicable.

REFERENCES

[1] J. Feng, “Improving sentiment analysis in literary texts through bidirectional encoder representations: A BERT-based approach,” Journal of Computational Methods in Sciences and Engineering, vol. 25, no. 5, pp. 4650-4664, 2025, doi: 10.1177/14727978251338004.

[2] Q. Zheng, T. Guo, G. Ding, H. Zhang, and K. Zhang, “Manufacturing service recommendation method based on knowledge graph and graph convolutional network,” Advanced Engineering Informatics, vol. 68, no. PA, pp. 103599-103599, 2025, doi: 10.1016/j.aei.2025.103599.

[3] S. Yang, F. Cao, K. Yu, and J. Liang, “Chain graphs structure learning given local background knowledge,” International Journal of Approximate Reasoning, vol. 186, pp. 109524-109524, 2025, doi: 10.1016/j.ijar.2025.109524.

[4] Y. Huang, R. Wang, Y. Li, G. Wang, and Y. Yan, “Knowledge graph-driven methodology for complex product archi-tecture solution generation and simulation verification,” Advanced Engineering Informatics, vol. 68, no. PA, pp. 103590-103590, 2025, doi: 10.1016/j.aei.2025.103590.

[5] J. Wang, Y. Chen, and Y. Li, “Evaluation and Feedback System for Physical Education Teaching Effec-tiveness Based on Artificial Intelligence,” International Journal of Computational Intelligence Systems, vol. 18, no. 1, pp. 303-303, 2025, doi: 10.1007/s44196-025-01046-5.

[6] Y. Han, H. Zhang, and Y. Man, “A method for constructing fault knowledge graphs based on an improved hidden Markov Model: A case study for papermaking industry,” Journal of Cleaner Production, vol. 520, pp. 146079-146079, 2025, doi: 10.1016/j.jclepro.2025.146079.

[7] N. Zhou, L. Sun, M. Han, and S. He, “PSA-GAT: Integrating position-syntax and cross-aspect graph atten-tion networks for aspect-based sentiment analysis,” Data & Knowledge Engineering, vol. 160, pp. 102477-102477, 2025, doi: 10.1016/j.datak.2025.102477.

[8] Q. Liu, S. Feng, and M. Huang, “TEQA: Temporal knowledge graph enhanced question answering,” Knowledge-Based Systems, vol. 325, pp. 113916-113916, 2025, doi: 10.1016/j.knosys.2025.113916.

[9] S. M. Hossain, “Emotional drivers of sustainable AI adoption: A sentiment analysis of early user feed-back on the deepSeek app,” Sustainable Futures, vol. 10, pp. 100947-100947, 2025, doi: 10.1016/j.sftr.2025.100947.

[10] M. Ramasamy and M. Elangovan, “Development of optimized cascaded LSTM with Seq2seqNet and transformer net for aspect-based sentiment analysis framework,” Web Intelligence, vol. 23, no. 3, pp. 295-318, 2025, doi: 10.3233/WEB-230096.

[11] X. Wang, Y. Cheng, P. Cheng, and X. Zhang, “AttDNet: An attribute-driven deep learning network for visual emotion analysis,” Pattern Recognition, vol. 171, no. PA, pp. 112098-112098, 2026, doi: 10.1016/j.patcog.2025.112098.

[12] J. You, H. Li, J. Deng, W. Li, Y. He, and F. Ren, “Hierarchical Reasoning Enhanced Few-Shot Multimodal Sentiment Analysis,” Neurocomputing, vol. 651, pp. 130883-130883, 2025, doi: 10.1016/j.neucom.2025.130883.

[13] F. Fischer, “Teaching Trump:Critical Issues in History and Civics Education,” Taylor & Francis, vol. 04, no. 08, pp. 16-18, 2025, doi: 10.4324/9781003494195.

[14] X. Guan, “Design and Application of a Teaching System Based on Mobile Internet,” International Journal of High Speed Electronics and Systems, vol. (prepublish), pp. 18-20, 2025, doi: 10.1142/S012915642540498X.

[15] B. Du, “The Introduction of Popular Music in Music Education Teaching

in Vocational Colleges," Journal of Education and Culture Studies, vol. 8, no. 4, pp. 18-20, 2024, doi: 10.22158/jecs.v8n4p183.

[16] C. Hajisoteriou, E. A. Solomou, and M. E. Antoniou, "Teaching history for global citizenship through an in-tercultural perspective," Frontiers in Education, vol. 9, pp. 1435402-1435402, 2024, doi: 10.3389/feduc.2024.1435402.

[17] G. O'Brien, "History repeating itself: an investigation of the challenges of teaching civic, social and political education," Irish Educational Studies, vol. 43, no. 4, pp. 1021-1042, 2024, doi: 10.1080/03323315.2023.2189134.

[18] X. Wu, "Exploration of Teaching Reform of Chinese Urban Construction History Course Based on Moral Education," Higher Education and Practice, vol. 1, no. 10, pp. 18-22, 2024, doi: 10.62381/H241A01.

[19] R. Göransdotter, "Looking Ahead: Nordic and British Perspectives on History of Education," History of Education Quarterly, vol. 64, no. 3, pp. 347-351, 2024, doi: 10.1017/heq.2024.27.

[20] A. K. Juyani, F. Zarei, and R. Maasoumi, "Efficacy of mobile-based educational intervention using Instruc-tional Systems Design in promoting preventive behaviors for sexually transmitted infections among Iranian women: A randomized controlled trial," BMC Public Health, vol. 24, no. 1, pp. 510-510, 2024, doi: 10.1186/s12889-024-18002-1.

[21] K. Zhang, "Design and application of intelligent teaching system for network and new media major driven by artificial intelligence technology," International Journal of Embedded Systems, vol. 17, no. 1-2, pp. 150-159, 2024, doi: 10.1504/IJES.2024.143759.

[22] A. Kruja, V. Ndrecaj, A. Çela, F. Morina, and E. Hysa, "Towards an Education for a Circular Economy: Mapping Teach-ing Practices in a Transitional Higher Education System," Sustainability, vol. 17, no. 21, pp. 9787-9787, 2025, doi: 10.3390/su17219787.

[23] M. K. Jones, "Centering Teaching and Learning Centers in Instructional Systems Design Conversations," TechTrends, vol. 66, no. 6, pp. 903-904, 2022, doi: 10.1007/s11528-022-00786-x.

[24] W. Chen, "Design of Music Teaching System Based on Artificial Intelligence," Mathematical Prob-lems in Engineering, vol. (1), Art. no. 2627395, 2022, doi: 10.1155/2022/2627395.

[25] G. Chen, "Design of College English Halving Classroom Teaching System Based on Big Data," Journal of Physics: Conference Series, vol. 2066, no. 1, pp. 18-19, 2021, doi: 10.1088/1742-6596/2066/1/012082.

[26] C. Duan, "Design of online volleyball remote teaching system based on AR technology," Alex-andria Engineering Journal, vol. 60, no. 5, pp. 4299-4306, 2021, doi: 10.1016/j.aej.2021.03.006.

[27] H. Dong, "Adapting during the pandemic: A case study of using the rapid prototyping instructional system design model to create online instructional content," The Journal of Academic Librarianship, vol. 47, no. 3, pp. 19-20, 2021, doi: 10.1016/j.acalib.2021.102356.